ACTA ASTRONOMICA
Vol. **44** (1994) pp. 165–189

The Optical Gravitational Lensing Experiment. The Optical Depth to Gravitational Microlensing in the Direction of the Galactic Bulge*

by

A. Udalski[1], M. Szymański[1], K. Z. Stanek[2,3], J. Kałużny[1], M. Kubiak[1], M. Mateo[4], W. Krzemiński[5], B. Paczyński[2] and R. Venkat[6]

[1] Warsaw University Observatory, Al. Ujazdowskie 4, 00–478 Warszawa, Poland
e-mail: (udalski,msz,jka,mk)@sirius.astrouw.edu.pl

[2] Princeton University Observatory, Princeton, NJ 08544–1001, USA
e-mail: (stanek,bp)@astro.princeton.edu

[3] N. Copernicus Astronomical Center, Bartycka 18, Warszawa 00-716, Poland

[4] Department of Astronomy, University of Michigan, 821 Dennison Bldg., Ann Arbor, MI 48109–1090, USA
e-mail: mateo@astro.lsa.umich.edu

[5] Carnegie Observatories, Las Campanas Observatory, Casilla 601, La Serena, Chile
e-mail: wojtek@roses.ctio.noao.edu

[6] Case Western Reserve University, 11896 Carlton Rd 440B, Cleveland, OH 44106, USA
e-mail: rxv8@po.cwru.edu

Received June 15, 1994

ABSTRACT

We present the analysis of the first two years of the OGLE search for gravitational lenses towards the Galactic bulge. We detected 9 microlensing events in an algorithmic search of $\sim 10^8$ measurements of $\sim 10^6$ stars. The characteristic time scales are in the range $8.6 < t_0 < 62$ days, where $t_0 = R_E/V$. The distribution of amplitudes is consistent with theoretical expectation. The stars seem to be drawn at random from the overall distribution of the observed bulge stars. We find that the optical depth to microlensing is larger than $(3.3 \pm 1.2) \times 10^{-6}$, in excess of current theoretical estimates.

Key words: *dark matter – gravitational lensing – stars: low-mass, brown dwarfs*

---

* Based on observations obtained at the Las Campanas Observatory of the Carnegie Institution of Washington.

1. Introduction

The Optical Gravitational Lensing Experiment (OGLE) is a long term project targeted at the determination of the rate and the statistical properties of gravitational microlensing of the Galactic bulge stars. The project was described by Udalski *et al.* (1992) and the first lensing events were reported by Udalski *et al.* (1993b, 1994a). All observations were done with the 1 meter Swope telescope at the Las Campanas Observatory, operated by the Carnegie Institution of Washington. The detector was a single Loral CCD with 2048 $\times$ 2048 pixels. We used a modified version of DoPhot photometric software (Schechter, Mateo and Saha 1993) to extract stellar magnitudes from the CCD frames.

The purpose of this paper is to present the first estimate of the optical depth to gravitational microlensing of the Galactic bulge stars. In the following sections we present the description of the selection criteria for microlensing event candidates, the scaling of the photometric errors as provided by the DoPhot, the analysis of the efficiency of recovering theoretical microlensing events, the event statistics and the overall discussion. This is largely a technical paper. The discussion of our results in the broader astronomical context will be provided elsewhere (Paczyński *et al.* 1994b).

The 13 fields covered with our CCD search in the 1992 and 1993 observing seasons are shown in Fig. 1. The complete list of microlensing event candidates is given in Table 1 in the chronological order of their maximum light t_{max} which is not the same as the order in which they were discovered in the data. The discovery order is given by the OGLE #, as listed.

Table 1

Properties of the OGLE microlensing events

Field	Lens Star #	N_t	N_c	V	$V-I$	t_{max} [JD]*	t_0	ϵ_{t0}	u	u_{max}	$P(\leq\epsilon)$	$P(\leq I)$	τ_k	OGLE #
BW3	I 161220	45	40	17.8	2.1	801.4	61.6	0.22	1.70	1.80	0.74	0.63	0.31	10
BW5	I 178651	27	25	20.7	1.6	805.5	45.5	0.21	0.17	0.65	0.39	0.81	0.67	2a
BWC	I 10648	33	33	20.7	1.6	804.1	49.2	0.21	0.27	0.62	...	...	...	2b
BW4	I 111538	6	6	20.8	1.5	806.9	13.5	0.12	0.23	0.58	0.21	0.91	0.40	4
MM7-A	I 86776	9	9	21.0	1.8	816.6	18.7	0.14	0.67	0.70	0.06	0.99	0.35	9
MM5-B	I 128727	13	11	19.6	1.5	818.8	8.6	0.08	0.35	0.74	0.52	0.40	0.35	6
BWC	I 120698	29	29	19.4	1.6	824.2	13.1	0.12	0.13	0.86	0.68	0.36	0.27	5
BW3	I 161225	12	12	17.6	1.7	830.6	11.2	0.10	1.15	1.81	0.58	0.43	0.13	3
BW7	I 117281	12	12	20.3	1.5	1153.5	24.8	0.22	0.45	0.68	0.40	0.68	0.41	1
BW8	I 198503	42	42	19.4	1.9	1178.9	55.9	0.28	0.38	1.21	0.47	0.18	0.44	7

*JD − 2448000

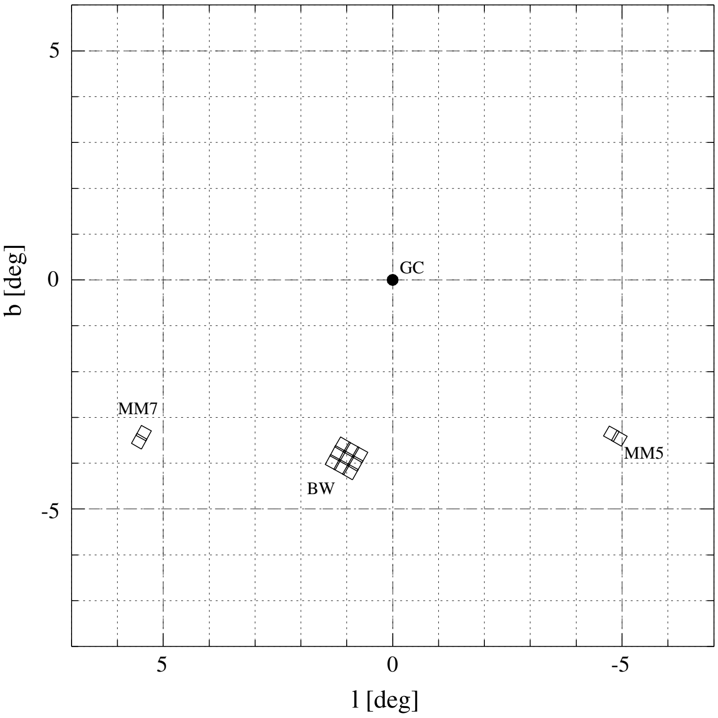

Fig. 1. Positions in the galactic coordinates of 13 fields in which a search for gravitational microlensing was carried out with the OGLE in 1992 and 1993 observing seasons.

2. The Lens Candidates

The first six OGLE microlensing events as reported by Udalski *et al.* (1993b, 1994a) were selected as follows. The observations were done in two observing seasons, 1992 and 1993, separated by 8 months during which no data was taken. First, the stars constant in season A (be it 1992 or 1993) were selected from the database of all I-band photometric measurements with additional requirement that $I \leq 19.5$ (Szymański and Udalski 1993). The procedure of defining a constant star is described in detail by Udalski *et al.* (1993a, p. 71-73; 1993b). In short, such a star must have at least $N = 12$ "good" measurements in the I band and a standard deviation from the mean less then the maximum allowed value σ_{max} for a given magnitude and a given field. There were $\sim 1.1 \times 10^6$ such stars in 1992 and $\sim 1.4 \times 10^6$ such stars in 1993. Next, the same stars were looked at in season B and those which had at least 5 measurements deviating from the A season average by more than $3\sigma_{max}$ were selected. Some additional filters were applied to reduce the number of objects. The remaining "variable" stars were all inspected and the six published events were selected according to a human judgment, not by a well defined algorithm. The judgment was relatively simple, as the vast majority of "variables" had very erratic, almost random changes in magnitude, most likely caused by some defects in the images. A few were long period variables. Only very "good looking" events were finally reported, those clearly standing above the noise.

In order to make a proper estimate of the optical depth to microlensing we have to know the efficiency of the OGLE system for the detection of microlensing events of various timescales. This requires a strictly algorithmic selection process to be used. Therefore, we changed a little the original selection criteria and supplemented them with a number of new ones, so as to reduce as much as possible the noise and to obtain the final, small number of lensing event candidates. Here is the final list of selection criteria used.

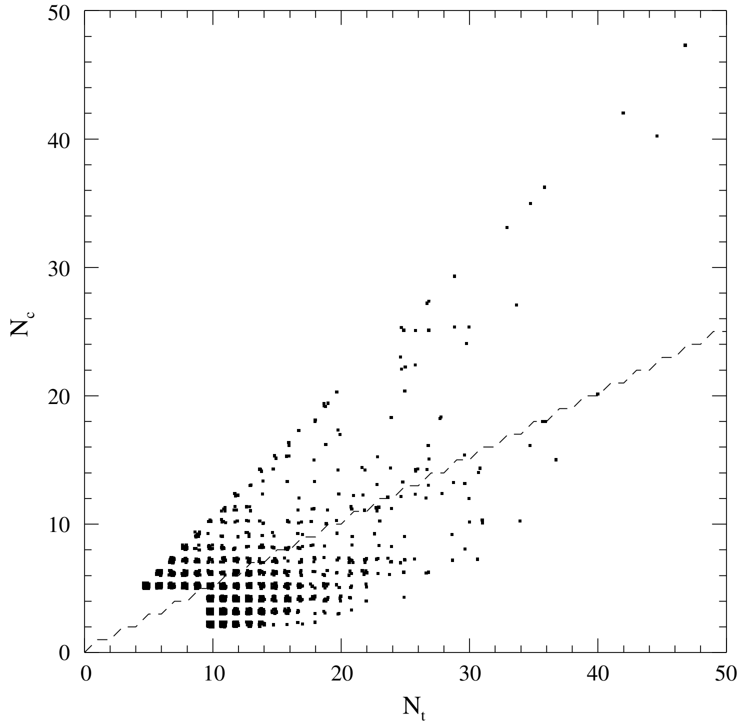

Fig. 2. The distribution of stars that were constant in one season and variable in the other season in the $N_t - N_c$ plane. The bigger the symbol the larger number of stars are at that location. N_t is the total number of measurements deviating *up* from the constant season average by more than 3 standard deviations; N_c is the maximum number of such measurements that are consecutive, *i.e.* with no non-deviating points between them. The dashed line corresponds to $N_c = 0.5N_t$. Stars below this line were excluded from further analysis.

For a star to be included in the search we required at least $N = 15$ good photometric measurements both in season A and B and at least 5 consecutive measurements in season B that deviated *up* in brightness by more than $3\sigma_{max}$ or at least 10 such points total. In addition, if the *total* number of such deviant points was N_t we required that at least $N_c \geq 0.5N_t$ such measurements be *consecutive*, *i.e.* we required at least N_c points to deviate *up*, with no "low" points in between. All stars that satisfied the preceding criteria had their data in season B blindly fitted to a microlensing light curve of a point mass lens, the magnitude at minimum light adopted as the mean magnitude in season A. There were three adjustable parameters of the model: the peak magnification A, the time of maximum light t_{max} and the characteristic time scale of the lensing event $t_0 = R_E/V$, where R_E is the Einstein ring radius and V is the relative transverse velocity in the source – lens – observer system (*cf* Paczyński 1986). Next, we required that there should be at least two data points within $3t_0$ on each side of t_{max} – this eliminated a number of "promising" light curves near the beginning or the end of each season, where the fitted maximum fell beyond the range covered by the observations. Then, the χ^2 was calculated twice, first with respect to the constant light level given by season A and next with respect to the "best fit" lensing curve; the ratio of the two was required to be in excess of 20.

The distribution of 2041 "variable" stars selected according to the original criteria is plotted in Fig. 2 in the $N_t - N_c$ diagram, together with a line separating them according to $N_c \geq 0.5N_t$. The condition $N_c \geq 0.5N_t$ reduced the sample to 469 stars. Next, we required that at least two points should be located on either side of the maximum – this reduced the sample to 336 stars. For these 336 objects the ratio of χ^2 given by the best fit lensing curve divided by χ^2 calculated with respect to a constant light *vs.* χ^2 of the fitted lens divided by the number of measurements N is shown in Fig. 3, together with the line separating the final 18 lensing candidates selected algorithmically.

The final step has been done by inspection of the original CCD frames to check if a particular lens candidate is not a result of some obvious defect, like a bleeding column. This has reduced the number of candidate events to 9, some of them redundant (OGLE #2a and OGLE #2b), as they were measured independently in the regions of overlap of adjacent CCD fields. All six lenses reported by Udalski *et al.* (1993b, 1994a) were recovered, as well as the double lens candidate (OGLE #7, Udalski *et al.* 1994b). Two new events, OGLE #9 and #10 have been found through the algorithmic search procedure[1]. These events, in particular #10, are not nearly as "good looking" as those reported in the past (Udalski *et al.* 1993b, 1994a). However, they came out of the algorithmic search, their CCD images were fine and there was no formal reason to reject them. One should be, however, aware that OGLE #10 might be in fact a very long period variable star.

The light curves for all final lens candidate events are shown in Fig. 4. It is important to note that the photometry we are using throughout this analysis and, in particular, the one shown in Fig. 4 is the photometry directly available from the database, while the light curves of the OGLE events published by Udalski *et al.* (1994a) were based on refined, differential photometry, as described in that paper.

[1] The OGLE lens numbering system is chronological. The event OGLE #8 has been discovered in another data set which is not analyzed in this paper.

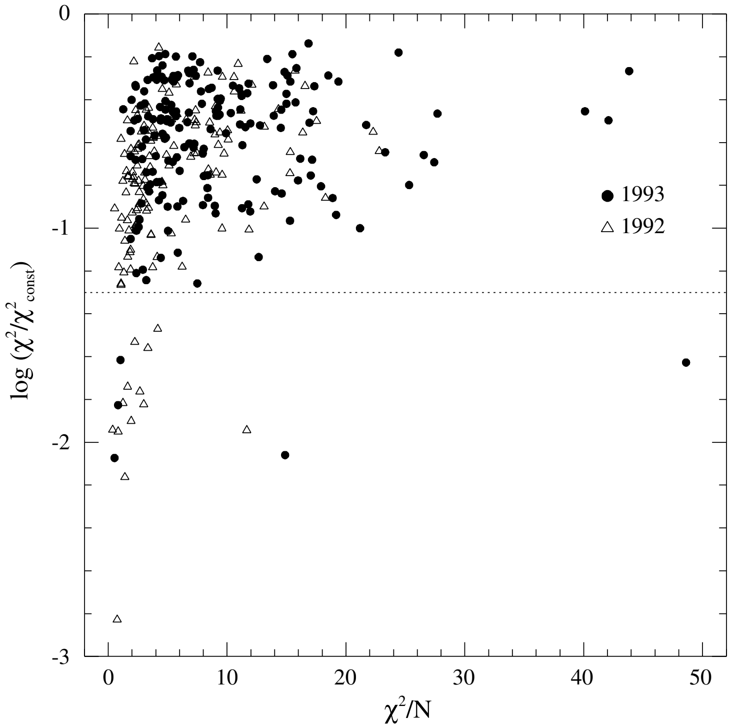

Fig. 3. The distribution of stars constant in one season and variable in the other in the χ^2 plane. χ^2 is the sum of squares of deviations from the best fit microlensing curve in units of the DoPhot errors. χ^2_{const} is the sum of squares of deviations from the constant season magnitude, also in units of the DoPhot errors. N is the number of good measurements in the "variable" season. Only the stars below the horizontal dashed line were selected for further analysis.

We use the database photometry as this is the only one available for all the stars on which the variety of tests are performed and we need a uniform approach to all stars in order to make an unbiased estimate of the optical depth.

All the events are listed in Table 1 which gives the field name, the star number in the database, the total number of measurements N_t that deviated up from the constant season average by more than $3\sigma_{max}$ threshold, the number N_c of such measurements that were consecutive, the photometric colors, the time of maximum, the event time scale t_0 and other parameters to be described in the subsequent sections. The last column lists the name of the event. Seven events were detected in the 1992 data, while the remaining two events were detected in the 1993 data. Notice that the number of stars searched for lensing was $\sim 1.4 \times 10^6$ in 1992 and $\sim 1.1 \times 10^6$ in 1993.

3. Scaling DoPhot Errors

The limiting magnitude of the OGLE photometry was always determined by the overlapping star images, never by the photon statistics and it was close to the

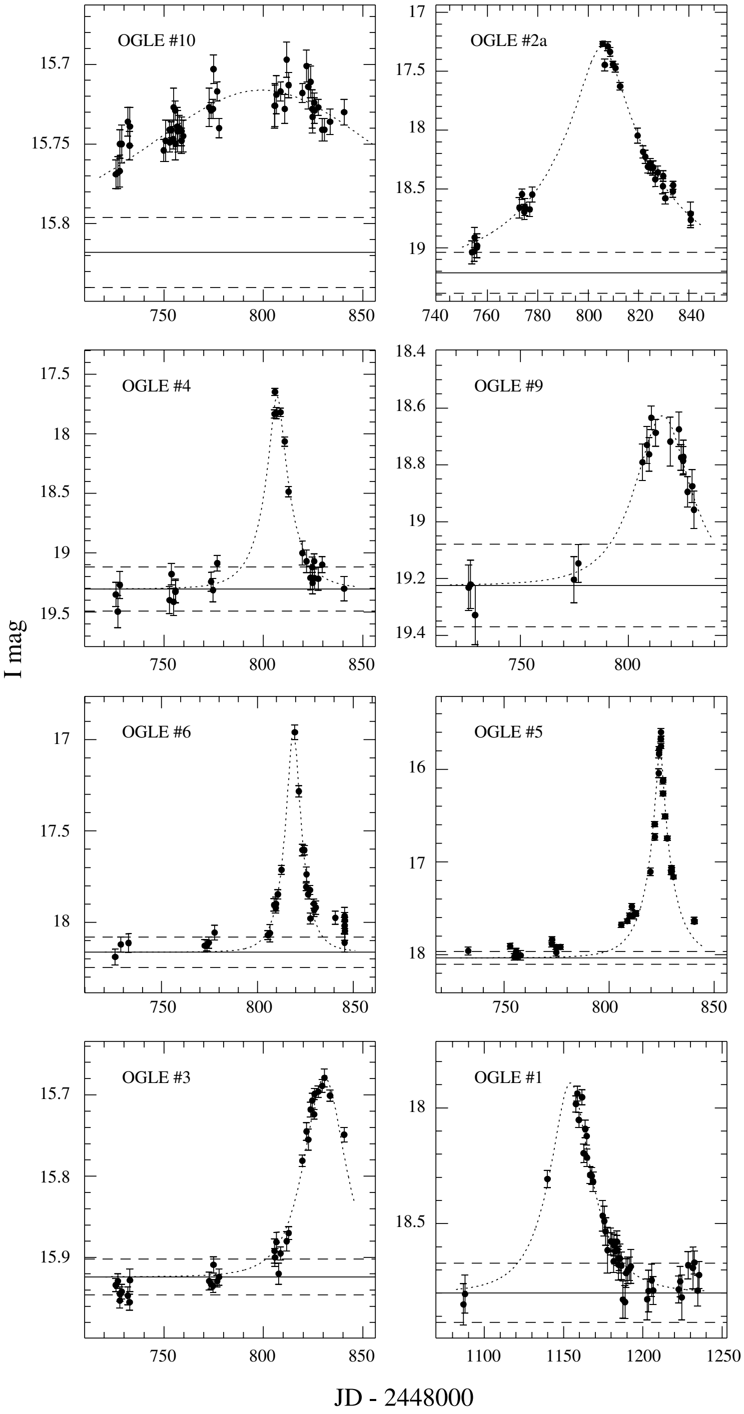

Fig. 4. The observed and theoretical (short dashed lines) light curves are shown for all events that were below the dashed horizontal line in Fig. 3 for which no obvious defects were found in the CCD frames. The solid horizontal lines show the level of average I magnitude in the observing season when the particular star was constant. The two horizontal dashed lines are separated from the solid lines by σ_{max} as described in Section 2.

turn-off point of the Bulge main sequence (Udalski *et al.* 1993a). Therefore, the observed luminosity function was rapidly increasing with the stellar magnitude, with most of the stars close to the detection limit and even more stars just below. It all implies that the photometric errors were not easy to estimate and many stars were unresolved blends of two or more stellar images. Naturally, we expect that the majority of the lensing candidates are to be found near the detection limit and we expect that the measurement errors at their minimum light are very difficult to estimate. The situation improves as the stellar image brightens during the event and dominates the background of faint and unresolved stars. In the following paragraphs we describe our attempt to estimate the errors of our photometry. However, it should be realized that there is only one way to obtain truly reliable photometry for the majority of our lensed stars at their minimum light: it is necessary to obtain images with a much smaller seeing, or in other words to move the detection limit by a few magnitudes below ours. At this time only HST can provide the required resolution.

It is important to find the relation between the errors as given by DoPhot and the real observational errors. To address this issue we have randomly chosen 1% of stars (in each of our 13 CCD fields) which were constant in the first or the second season: $\sim$ 11 000 in 1992 and $\sim$ 14 000 in 1993 and we used them for a variety of tests. We shall refer to these as the template stars. Next, we selected those template stars which had a total of at least 40 photometric measurements made in the two observing seasons – there were $\sim$ 25 000 such stars and we used the measurements from both seasons for all those stars in the following analysis.

For every star we calculated the DoPhot error-weighted average I-magnitude according to:

$$\bar{I} = \sum_i \frac{I_i}{\sigma_{i,D}} / \sum_i \frac{1}{\sigma_{i,D}} \tag{1}$$

where $\sigma_{i,D}$ is the DoPhot error of the measurement number i. The individual deviations were calculated as $(I_i - \bar{I})/\sigma_D$. These deviations were grouped according to the values of σ_D and $\bar{I}$. The cells with the number of deviations exceeding 2 000 were used to obtain scaling factor between the DoPhot and the real error as a function of σ_D and $\bar{I}$. The procedure is described in detail by Lupton *et al.* (1989), p. 206, so here we give only its brief outline. From each cell with more than 2 000 measurements we have randomly selected $m = 2\,000$ measurements for the analysis so as to have a uniform statistics. The 2 000 deviations within a given cell were sorted according to the distance from the mean within the cell and the dispersion of the deviations was calculated. Next, we removed the deviations farthest from the mean and we recomputed the dispersion. The whole procedure was repeated to obtain $s(m, n)$, the dispersion of deviations as a function of n, the number of stars remaining. Next, the same process was repeated for deviations drawn randomly from a gaussian normal distribution and obtained by a series of Monte Carlo simulations.

An example of $s(m,n)$ for both real and simulated data is shown in Fig. 5. In the logarithmic plot the curves representing the two dispersions are parallel up to a certain value of n beyond which the real data sample is contaminated by variable stars as well as a variety of defects in the CCD frames. This means the DoPhot error σ_D may represent the real observational error provided it is multiplied by an appropriate scaling factor F which in the case shown in Fig. 5 is $F = 1.48$ and

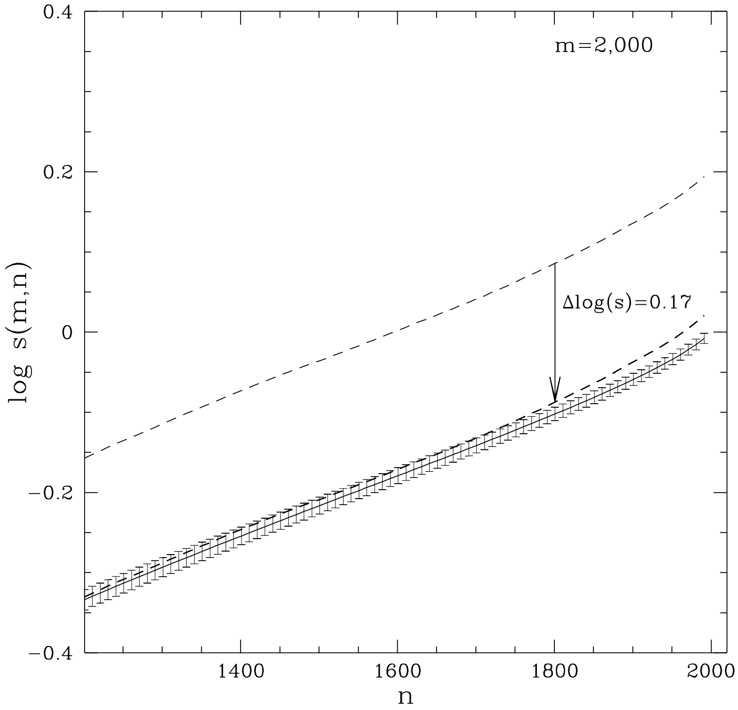

Fig. 5. The variation of the variance $s(m,n)$ as a function of the number of measurements n remaining in the sample of originally $m = 2\,000$ measurements. The upper dashed line is based on real OGLE data with the DoPhot errors and the I-band magnitudes in the ranges $0.016 < \sigma_D \le 0.024$ and $17.68 < \bar{I} \le 17.83$, respectively. The solid line corresponds to a theoretical relation for a gaussian distribution with a standard deviation $\sigma = 1.0$. The error bars along the solid line correspond to one standard deviation as estimated from a large number of Monte Carlo simulations. The lower dashed line is just the upper line shifted down by 0.17 in the $\log s$ which corresponds to the scaling factor $F = 1.48$, as described in the text. Notice that for $n \ge 1\,800$ the down-shifted dashed line deviates upwards from the theoretical line. This indicates that there is a $\sim 10\%$ non-gaussian tail of the OGLE errors.

corresponds to the average distance between the two parallel curves. The same procedure was used to obtain the scaling factor for all $(\sigma_D, \bar{I})$ cells with more than 2 000 deviations. For the cells with fewer than 2 000 deviations the average scaling factor $F = 1.29$ was adopted. The values of F-factors are listed in Table 2 as a function of $\bar{I}$ and σ_D for each cell which had more than 2 000 measurements in it. The number of measurements per cell is given in Table 3.

Table 2

F-corrections for constant stars sample

$\bar{I}$	$\sigma_D <$											
	0.005	0.007	0.011	0.016	0.024	0.035	0.052	0.077	0.114	0.169	0.250	0.500
13.750	...	...	...	...	...	...	...	...	...	...	...	...
13.875	...	...	...	...	...	...	...	...	...	...	...	...
14.000	...	...	...	...	...	...	...	...	...	...	...	...
14.125	...	...	...	...	...	...	...	...	...	...	...	...
14.250	...	...	...	...	...	...	...	...	...	...	...	...
14.375	...	...	...	...	...	...	...	...	...	...	...	...
14.500	...	...	...	...	...	...	...	...	...	...	...	...
14.625	...	...	...	...	...	...	...	...	...	...	...	...
14.750	...	...	...	...	...	...	...	...	...	...	...	...
14.875	...	...	...	...	...	...	...	...	...	...	...	...
15.000	...	...	...	...	...	...	...	...	...	...	...	...
15.125	...	1.344	1.087	...	...	...	...	...	...	...	...	...
15.250	...	1.330	1.134	...	...	...	...	...	...	...	...	...
15.375	...	1.502	1.167	1.017	...	...	...	...	...	...	...	...
15.500	...	1.443	1.240	0.975	...	...	...	...	...	...	...	...
15.625	...	1.461	1.220	1.058	...	...	...	...	...	...	...	...
15.750	...	...	1.337	1.073	...	...	...	...	...	...	...	...
15.875	...	...	1.202	1.105	...	...	...	...	...	...	...	...
16.000	...	...	1.273	1.043	...	...	...	...	...	...	...	...
16.125	...	...	1.255	1.104	...	...	...	...	...	...	...	...
16.250	...	...	1.396	1.201	...	...	...	...	...	...	...	...
16.375	...	...	1.470	1.253	...	...	...	...	...	...	...	...
16.500	...	...	1.579	1.349	...	...	...	...	...	...	...	...
16.625	...	...	...	1.260	1.140	...	...	...	...	...	...	...
16.750	...	...	...	1.317	1.160	...	...	...	...	...	...	...
16.875	...	...	...	1.389	1.087	...	...	...	...	...	...	...
17.000	...	...	...	1.388	1.194	...	...	...	...	...	...	...
17.125	...	...	...	1.374	1.142	1.100	...	...	...	...	...	...
17.250	...	...	...	1.432	1.318	1.212	...	...	...	...	...	...
17.375	...	...	...	1.550	1.394	1.281	...	...	...	...	...	...
17.500	...	...	...	...	1.332	1.183	...	...	...	...	...	...
17.625	...	...	...	...	1.415	1.240	...	...	...	...	...	...
17.750	...	...	...	...	1.487	1.226	1.211	...	...	...	...	...
17.875	...	...	...	...	1.471	1.405	1.226	...	...	...	...	...
18.000	...	...	...	...	1.550	1.419	1.307	...	...	...	...	...
18.125	...	...	...	...	...	1.534	1.320	1.453	...	...	...	...
18.250	...	...	...	...	...	1.458	1.358	1.215	...	...	...	...
18.375	...	...	...	...	...	1.515	1.358	1.284	...	...	...	...
18.500	...	...	...	...	...	1.648	1.432	1.295	1.292	...	...	...
18.625	...	...	...	...	...	1.756	1.442	1.141	1.239	...	...	...
18.750	...	...	...	...	...	...	1.397	1.200	1.154	...	...	...
18.875	...	...	...	...	...	...	1.447	1.170	1.124	1.310	...	...
19.000	...	...	...	...	...	...	1.580	1.118	1.064	1.176	...	...
19.125	...	...	...	...	...	...	1.559	1.254	0.954	1.095	...	...
19.250	...	...	...	...	...	...	1.603	1.120	0.938	1.084	...	...
19.375	...	...	...	...	...	...	...	1.306	0.848	0.939	1.183	...
19.500	...	...	...	...	...	...	...	1.425	1.201	1.009	1.206	...
19.625	...	...	...	...	...	...	...	...	1.321	1.264	...	...
19.750	...	...	...	...	...	...	...	...	...	...	...	...

Table 3

Number of measurements per cell

$\bar{I}$	$\sigma_D <$											
	0.005	0.007	0.011	0.016	0.024	0.035	0.052	0.077	0.114	0.169	0.250	0.500
13.750	0	10	20	14	3	0	0	0	0	0	0	0
13.875	6	71	52	44	2	0	0	0	0	0	0	0
14.000	36	261	230	175	51	1	0	0	0	0	0	0
14.125	59	479	400	282	33	0	0	0	0	0	0	0
14.250	98	924	828	413	16	0	0	0	0	0	0	0
14.375	107	992	851	366	18	0	0	0	0	0	0	0
14.500	118	1231	1083	412	2	0	0	0	0	0	0	0
14.625	86	1141	1004	404	2	0	0	0	0	0	0	0
14.750	77	1257	1323	607	5	0	0	0	0	0	0	0
14.875	84	1285	1349	687	17	7	0	0	0	0	0	0
15.000	116	1879	1979	1009	47	1	0	0	0	0	0	0
15.125	121	3014	3416	1594	24	0	0	0	0	0	0	0
15.250	81	2744	3648	1815	55	2	0	0	0	0	0	0
15.375	61	3390	5011	2652	47	1	0	0	0	0	0	0
15.500	21	2866	5037	3056	87	0	0	0	0	0	0	0
15.625	12	2591	4972	3006	160	2	0	0	0	0	0	0
15.750	3	1727	4676	3605	177	12	0	0	0	0	0	0
15.875	1	1222	4000	2994	109	0	0	0	0	0	0	0
16.000	0	926	4268	3880	161	0	0	0	0	0	0	0
16.125	0	629	4326	4816	297	0	0	0	0	0	0	0
16.250	0	230	3394	5680	703	18	0	0	0	0	0	0
16.375	0	150	2763	5680	863	17	0	0	0	0	0	0
16.500	0	50	2110	6963	1449	31	0	0	0	0	0	0
16.625	0	11	1588	7727	2016	91	0	0	0	0	0	0
16.750	0	2	808	7418	2999	167	0	0	0	0	0	0
16.875	0	0	312	7069	4268	505	7	0	0	0	0	0
17.000	0	0	162	5908	4906	762	1	0	0	0	0	0
17.125	0	0	44	6036	7613	2029	45	0	0	0	0	0
17.250	0	0	11	4327	9218	3007	86	0	0	0	0	0
17.375	0	0	1	2950	12059	5704	244	0	0	0	0	0
17.500	0	0	0	1451	11885	8961	764	6	0	0	0	0
17.625	0	0	0	553	11219	12912	1645	17	0	0	0	0
17.750	0	0	0	212	8406	18443	4005	148	21	0	0	0
17.875	0	0	0	54	5606	24812	8069	438	35	0	0	0
18.000	0	0	0	21	3309	27890	13705	1217	30	0	0	0
18.125	0	0	0	0	1466	29491	23916	3589	68	0	0	0
18.250	0	0	0	0	384	22682	33448	8036	382	12	0	0
18.375	0	0	0	0	85	16085	44656	15667	892	9	0	0
18.500	0	0	0	0	27	9771	51801	27019	3091	120	0	0
18.625	0	0	0	0	1	4629	53754	44199	7971	286	25	9
18.750	0	0	0	0	0	1651	42779	59558	15629	747	25	0
18.875	0	0	0	0	0	497	30604	69514	25459	2334	92	6
19.000	0	0	0	0	0	102	17199	79236	46688	7608	424	47
19.125	0	0	0	0	0	16	7527	70903	66150	15318	978	69
19.250	0	0	0	0	0	3	2726	51196	73382	22520	1797	111
19.375	0	0	0	0	0	1	579	26562	64543	28735	3399	146
19.500	0	0	0	0	0	0	76	8631	38148	25192	3903	100
19.625	0	0	0	0	0	0	1	915	6021	4635	894	30
19.750	0	0	0	0	0	0	0	57	558	426	45	0

Fig. 5 can also be used to estimate the fraction of measurements that correspond to either variable or "defective" star images. The $s(m, n)$ curve for the real data deviates from the simulated one at about $n = 1\,800$, which indicates that roughly 10% of all measurement are non-gaussian for whatever reason. It seems likely that the vast majority of these "variables" are spurious, indicative of severe crowding and a variety of CCD defects. It is worth noticing that the same analysis when performed for all stars in the database of Szymański and Udalski (1993) revealed $\sim 30\%$ of non-gaussian measurements. This indicates that the procedure of pre-selecting constant stars removed most of the noise from the data. Unfortunately, even the $\sim 10\%$ contamination of the measurements of constant stars by the non-gaussian tail does not allow us to use rigorous χ^2 tests to assess the quality of agreement between the candidate lensing events and the best fit theoretical curves.

As a by-product of finding the scaling factors we also found a relation between the DoPhot errors and the stellar magnitude. For each bin of the I magnitude we found the most common value of σ_D in Table 3 and we fitted the relation with the simple formula:

$$\sigma_{D,I_1} \approx \sigma_{D,I_2} 10^{(I_1 - I_2)/3.5} \tag{2}$$

which allows us to estimate how the measurement error scales with stellar brightness. This is important in the models of lensing events. According to Eq. (2) when a star brightens from I_2 to I_1 by 3.5 magnitudes then its DoPhot error decreases by a factor ~ 10. This relation will be used in our Monte Carlo estimate of the OGLE microlensing detection efficiency.

4. The Efficiency of Recovery of Microlensing Events

The efficiency of the algorithmic search procedure described in Section 2 was tested with $\sim$ 14 000 stars in 1992 and with $\sim$ 11 000 stars in 1993. The template stars were not necessarily constant in the test season as they were selected as constant in the other season. They provided the time sequences of measurements and their DoPhot errors. For every value of event time scale t_0 we generated 100 000 Monte Carlo simulations of microlensing events. The star to be microlensed was randomly selected each time and the dimensionless impact parameter p/R_E and the time of peak magnification t_{max} were randomly selected from the uniform distributions: $0 \leq p/R_E \leq 2$, $0 \leq t_{max} \leq 1$ yr. R_E is the Einstein ring radius and $t_{max} = 0$ corresponded to either 1992.0 or 1993.0, for the two observing seasons, respectively. The simulations were done for 61 values of t_0 in the range $-1 \leq \log t_0 \leq 2$ (days).

The data points for simulated events were obtained as follows. First, theoretical magnitude I_t was calculated from a model for every value of time for which a real measurement and its DoPhot error were available, I_{obs}, $\sigma_{D,obs}$. Next, the DoPhot error $\sigma_{D,t}$ was assigned to the theoretical magnitude by rescaling the observational error $\sigma_{D,obs}$ according to the magnitude difference $I_t - I_{obs}$ and following Eq. (2).

The "true" theoretical error was calculated as $\sigma_t = \sigma_{D,t} \times F$, where the scaling factor was obtained from Table 2 according to the values of I_t and $\sigma_{D,t}$. Finally, the "actual" theoretical error was obtained with the Monte Carlo simulation using gaussian distribution with the standard deviation given as σ_t and this "actual" error was added to the theoretical magnitude I_t to obtain the simulated data point I_s. This procedure was repeated to generate a series of simulated data points for every time at which there was an actual measurement available. The full series of simulated data points was treated in the same way as a series of real observations and the algorithm described in Section 2 was used for detection of the model event. Four examples of simulated events are shown in Fig. 6.

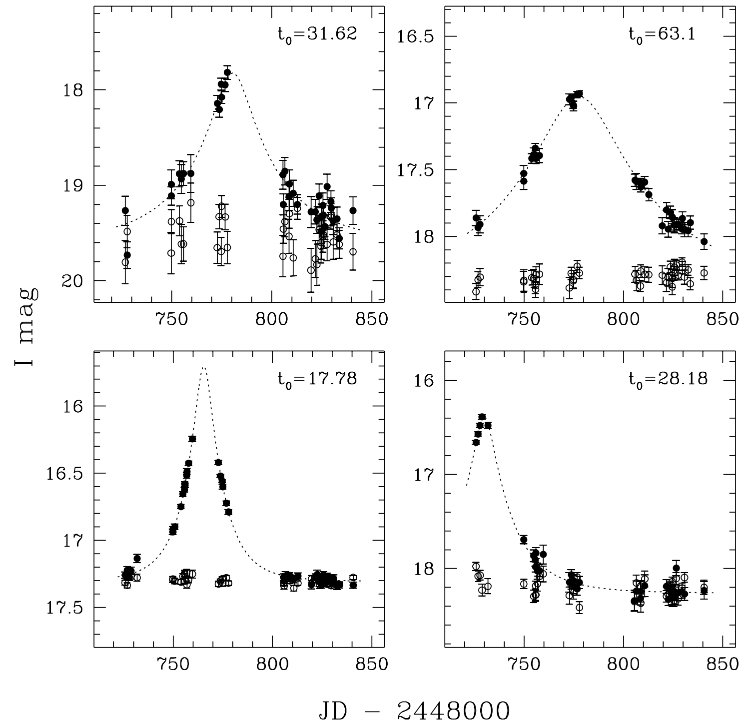

Fig. 6. Four examples of template star measurements are shown with open circles and the four simulated microlensing events are shown with filled circles and short dashed lines.

The fraction of events that have passed the detection criteria was multiplied by a factor of two and adopted as the OGLE efficiency to detect events of a given time scale t_0. This factor comes from the fact that the traditional definition of the optical depth requires the source to be within one Einstein radius of the lens, i.e. only the events with the dimensionless impact parameters smaller than unity, $p/R_E \leq 1$ are counted, while our simulations covered a region twice as large, $p/R_E \leq 2$. Imagine that we were able to recover *all* events with $p/R_E \leq 1$ and none with a larger impact parameter. In this case 50% of all simulated events would be detected but the OGLE efficiency would be 100%.

The OGLE detection criterion is expressed in terms of measurement errors rather than the event magnification. A low amplitude event may be detected if the source is bright and the errors are small, like the OGLE #3 for which $p/R_E = 1.08$, whereas a microlensing of a very faint star may be detectable only for $p/R_E \ll 1$. If the OGLE experiment had no gaps in the data, the observations were carried out for 12 months every year and we were able to recover all events with $p/R_E \leq 2$ then our sensitivity would be equal 2. Of course, in that case we would have to extend our simulations to larger impact parameters until we reach so low magnifications that the model events are no longer recoverable.

The OGLE observing season lasted about 4 months every year with large gaps in the coverage caused by the telescope scheduling and the weather conditions. Hence, the sensitivity was never even close to 1 not to mention 2. The plots of the efficiency as a function of event timescale is shown in Fig. 7 for the 1992 and 1993 seasons with the solid and dashed lines, respectively. The two lines are rather close to each other. The efficiency drops rapidly for t_0 shorter than a few days as the stars were never observed more than twice a night. The efficiency approaches $\sim 30\%$ for long timescales which is approximately the fraction of each year covered by the OGLE observing season. Please note that at present we do not investigate the efficiency of recovery of the very long lasting events with $t_0 > 1$ yr, as those would be classified as variable stars in both 1992 and 1993. We plan to investigate those long timescales when the data covering many years becomes available.

5. The Event Statistics

Because of distinctly non-gaussian distribution of the OGLE measurement errors even for the stars selected as constant, we cannot use the standard χ^2 test to assess the goodness of fit between the observed luminosity variations of the microlensing candidate events. Therefore, we have to make other checks of the statistical properties we expect of genuine lensing events. The following test is equivalent to a comparison between the observed distribution of event amplitudes and the distribution expected theoretically. The next two tests are designed to verify the expectation that all Galactic bulge stars are equally likely to be microlensed.

5.1. $p/p_{max} = u/u_{max}$ *Statistics*

A question frequently asked is: do OGLE events have the expected distribution of peak magnifications? This cannot be answered directly as the detection threshold is very fuzzy. Instead, we may use a criterion similar to the $\langle V/V_{max} \rangle$ originally proposed by Schmidt (1968) to study quasar distribution.

For every candidate event the best fit provides a value of the dimensionless impact parameter, $u \equiv p/R_E$ and that is directly related to the peak magnification A:

$$A = \frac{u^2 + 2}{u\sqrt{u^2 + 4}} \tag{3}$$

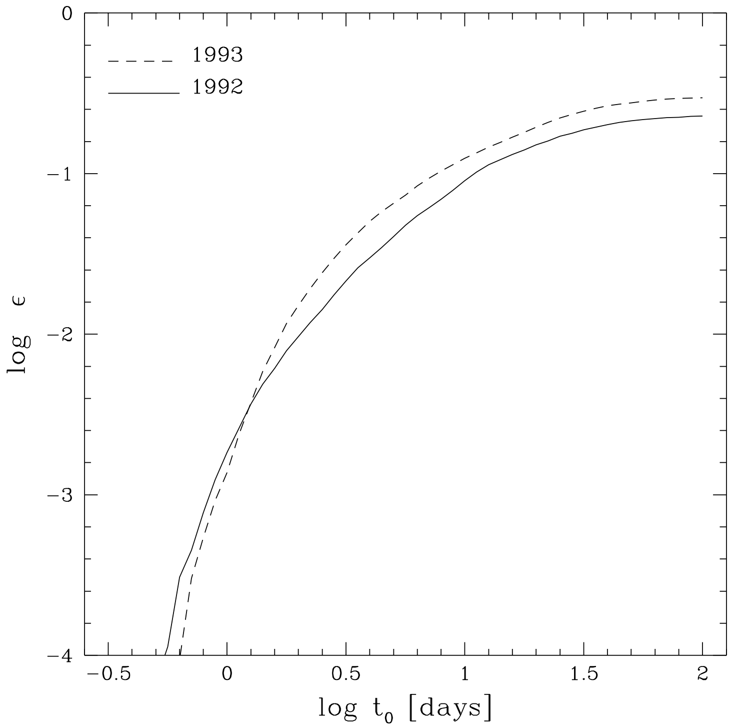

Fig. 7. The sensitivity of the OGLE microlensing search ϵ is shown as a function of the event timescale t_0 for the two observing seasons. Notice the abrupt drop in sensitivity for timescale below few days and the leveling off at $\sim 30\%$ for long timescale events.

(*e.g.* Paczyński 1986). Given the particular lens case with its distribution of measurements and errors we may ask a question: what is the maximum impact parameter u_{max} for which this event would have passed our algorithmic detection criteria as described in Section 2? Of course, the larger the impact parameter the lower the magnification and the closer are all measurements to the baseline magnitude.

Following the description given in Section 4 a series of simulated events was generated with all lens parameters kept constant, except for the dimensionless impact parameter u. The procedure was repeated until the maximum value u_{max} was found; this corresponded to the detection threshold of the event. As the test events were Monte Carlo simulated there was not a discontinuous jump from full detectability for $u \leq u_{max}$ to none above u_{max}. Rather, the fraction of model events that were detected varied fairly rapidly but smoothly with u. Therefore, the u_{max} was defined with the integral formula

$$u_{max} = \int_0^\infty f_d(u)\,\mathrm{d}u \tag{4}$$

where $f_d(u)$ is the fraction of events detected as a function of the impact parameter. Naturally, in practice there was never any need to extend the integral to infinity as the detectability $f_d(u)$ approached zero very rapidly as soon as the impact parameter exceeded u_{max}.

The lens trajectory with respect to the source is expected to be random. Thus, a detectable lens has its impact parameter uniformly distributed in the interval $0 \leq u \leq u_{max}$ and therefore we expect that u/u_{max} should be uniformly distributed in the range (0,1). Notice that the specific value of u_{max} has to be determined for each event individually as every event has a unique time sequence of measurements and errors. Nevertheless, we expect all events to share the property that their u/u_{max} parameters should be uniformly but randomly distributed in the (0,1) interval. Indeed, we find that u/u_{max} is uniformly distributed as expected for random impact parameters – this point will be discussed in Subsection (5.4)

The situation is somewhat more complicated if a lens is double. In this case a concept of positive and negative impact parameter has to be introduced and the actual impact parameter is expected to be uniformly distributed in the range $u^- \leq u \leq u^+$, where u^- and u^+ are the minimum and the maximum values for which the lens can be detected. One of our events, OGLE #7, has a very dramatic light curve and it is likely to be caused by a double lens (Udalski *et al.* 1994b). In this particular case the absolute values of u^- and u^+ are about equal and it makes sense to use the u/u_{max} parameter. Another possibly double lens, OGLE #6 (Mao and DiStefano 1994), is not so dramatic and for the purpose of the current analysis we treat it as a single lens case.

The best fit dimensionless impact parameters, u, and the maximum dimensionless impact parameters u_{max} are listed in Table 1 for all OGLE events. For the purpose of this analysis we treated OGLE #7 as a single lens, thus all its parameters given in Table 1 should be treated as crude estimates only. A full double lens analysis will be presented elsewhere (Udalski *et al.* 1994b).

5.2. Detectability Distribution

Now we have to check if the lensed stars are random or they have some common properties which might indicate that the variability has something to do with the star. Gravitational lensing should affect all Galactic bulge stars with the same probability.

In this Subsection we check if the lens candidates are randomly distributed in terms of their "detectability". Let us take a specific OGLE event #k, where $k = 1, 2, 3, 4, 5, 6, 7, 9, 10$, with its specific timescale $t_{0,k}$ and its dimensionless impact parameter u_k. For every event we repeated our sensitivity test as described in Section 4 for the specific values of $t_{0,k}$ and u_k. We made 200 simulations for each of the $\sim$ 14 000 template stars which were selected as constant in 1993 to test them for the "detectability" of OGLE lenses # 2, 3, 4, 5, 6, 9 and 10 in the 1992 data. We also made 200 simulations for each of the $\sim$ 11 000 template stars which were selected as constant in 1992 to test them for the "detectability" of OGLE lenses #1 and 7 in the 1993 data.

In addition we made 4 000 simulations for each star which was observed as the candidate event OGLE #k with its time scale $t_{0,k}$. For every star, including the one that had undergone the event, we calculated the fraction $\epsilon_i = N_{r,i}/N_{t,i}$. $N_{t,i}$ is the total number of simulated events for the star number i; $N_t = 200$ for test stars and $N_t = 4\,000$ for the event star. $N_{r,i}$ is the number of cases in which a theoretical event has been recovered for the star number i. We followed the procedure described in Section 2 to "detect" these theoretical events. The larger the value of ϵ_i the easier it was to recover the events, *i.e.* the "better" was the star.

Now, we rank order stars according to the value of their ϵ_i parameter and we establish a cumulative recovery probability as a function of ϵ, the efficiency of detection:

$$P(\leq \epsilon) = \sum_{i,(\epsilon_i \leq \epsilon)} \epsilon_i / \sum_i \epsilon_i \tag{5}$$

$P(\leq \epsilon)$ is the probability that an event with the timescale $t_{0,k}$ and the dimensionless impact parameter u_k is discovered among the stars for which the discovery efficiency is less or equal ϵ. Finally, we calculated $P(\leq \epsilon_k)$, where ϵ_k was the recovery fraction for the actual OGLE #k event, the one we were analyzing. If its selection was fair then the value of $P(\leq \epsilon_k)$ should have a uniform probability distribution in the interval (0,1). The values of $P(\leq \epsilon_k)$ are listed in Table 1. The relations between $P(\leq \epsilon)$ and ϵ are shown for all OGLE events in the nine panels of Fig. 8. The vertical dashed lines correspond to the the value of ϵ_k for each lens.

5.3. I Magnitude Distribution

We followed a similar procedure to find out if the candidate events were randomly but uniformly distributed in the I magnitude of our sample. For every template star we had the value of its magnitude I_i and its efficiency parameter for the lens detectability ϵ_i. The value of ϵ_i was specific to every OGLE event, as described in previous Subsection. We rank ordered all stars according to their I_i magnitude and we calculated

$$P(\leq I) = \sum_{i,(I_i \leq I)} \epsilon_i / \sum_i \epsilon_i \tag{6}$$

where $P(\leq I)$ is the probability that an event with the time scale $t_{0,k}$ is discovered among stars brighter than I. The value corresponding to the event OGLE #k is $P(\leq I_k)$, where I_k is its baseline magnitude. If the selection was fair then the value of $P(\leq I_k)$ should be uniformly but randomly distributed in the interval (0,1). The values of $P(\leq I_k)$ are listed in Table 1. The relations between $P(\leq I)$ and I are shown for all OGLE events in the nine panels of Fig. 9. The vertical dashed lines correspond to the the value of I_k for each lens.

The efficiency of lens detectability ϵ is in general higher for bright stars because their measurements have smaller errors, so we expect that the last two distribution

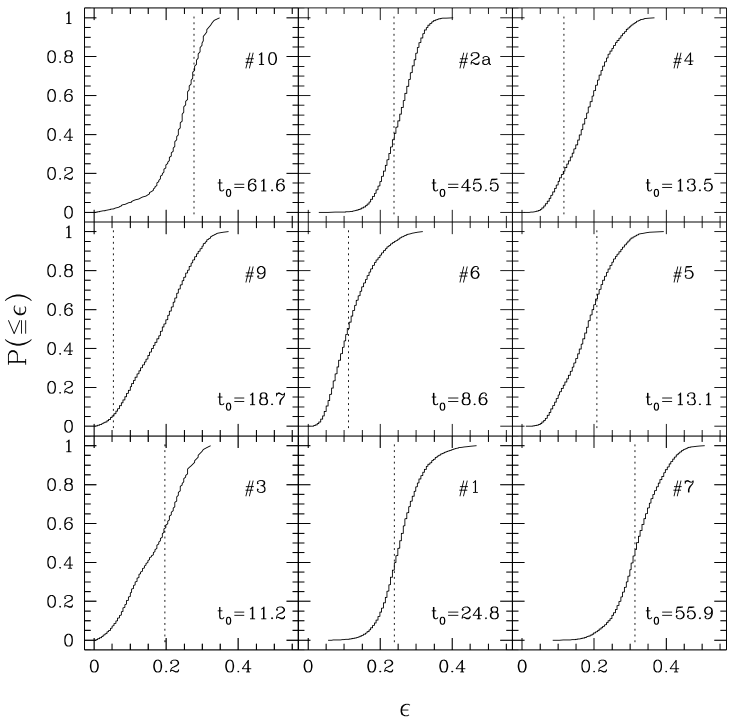

Fig. 8. The distributions of cumulative probability $P(\leq \epsilon)$ for the detection of a lensing event of a given time scale t_0 is shown as a function of the detection efficiency ϵ for $\sim$ 11 000 template stars in 1992 and $\sim$ 14 000 template stars in 1993. Each panel corresponds to a different lensing event and its time scale t_0. The efficiency of detection for each event is indicated with a vertical dashed line.

tests are somewhat related. The correlations between the values of ϵ and I magnitude is shown in nine panels in Fig. 10 for the nine lens candidate events. Notice that while in many cases the correlation is strong it is either weak or absent in some cases. In general, it is clear that each lens has a different detectability pattern among the stars.

5.4. Overall Distribution Properties

The results of the three preceding tests are conveniently displayed in three panels in Fig. 11. The distribution of all three parameters should be uniform and random in the range (0,1) and it seems to be such. With the small number of events there is no point to apply a sophisticated statistical analysis – it is clear that there are no significant departures from the expected distribution. In other words, we have no reason to doubt that the 9 events presented in this paper are not due to gravitational microlensing.

Still, one may notice that there are no events in the middle panel of Fig. 11 for $0.75 \leq P(\leq \epsilon) \leq 1.0$ and none in the lower panel for $0.0 \leq P(\leq I) \leq 0.17$. These two are correlated as explained in the previous sub-section: bright stars have

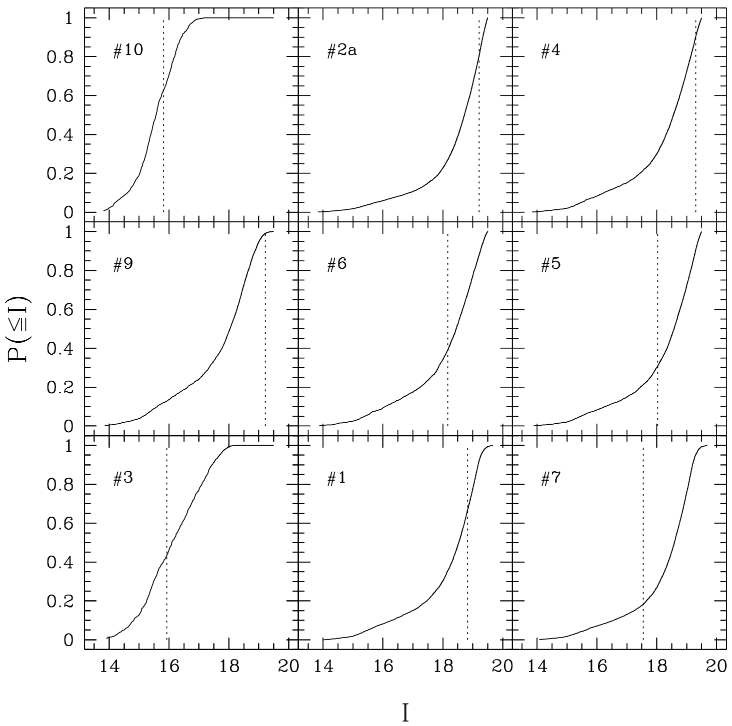

Fig. 9. The distributions of cumulative probability $P(\leq I)$ for the detection of a lensing event of a given time scale t_0 is shown as a function of I-magnitude for $\sim$ 11 000 template stars in 1992 and $\sim$ 14 000 template stars in 1993. Each panel corresponds to a different lensing event and its time scale t_0. The I-magnitude for each event is indicated with a vertical dashed line.

higher efficiency for lens detection. The gaps are not statistically significant, but they may be partly due to a relatively large contribution of the Galactic disk at the bright end. Disk stars make $\sim$ 50% of all stars brighter than $V = 15$ and $\sim$ 20% of all stars brighter than $V = 18$. We have not excluded them from the search. We did not expect any lensing events among them and we found none. This absence may contribute to the apparent gaps in the distribution in the middle and the lower panels of Fig. 11.

5.5. Color Distribution

We cannot easily test the distribution in $V - I$ colors, as the database of stars for which good $V - I$ color are known is about three times smaller than the I magnitude database. The reason is simple: most stars are close to the detection limit and due to large reddening of the Galactic bulge many of them have only I magnitude well measured while only some have both. Nevertheless, a qualitative impression of a random distribution is apparent when the locations of the OGLE lensed stars are plotted in the color-magnitude diagram, as shown in Fig. 12. The positions of $\sim$ 12 000 stars are plotted, 2.5% of the whole database for which we

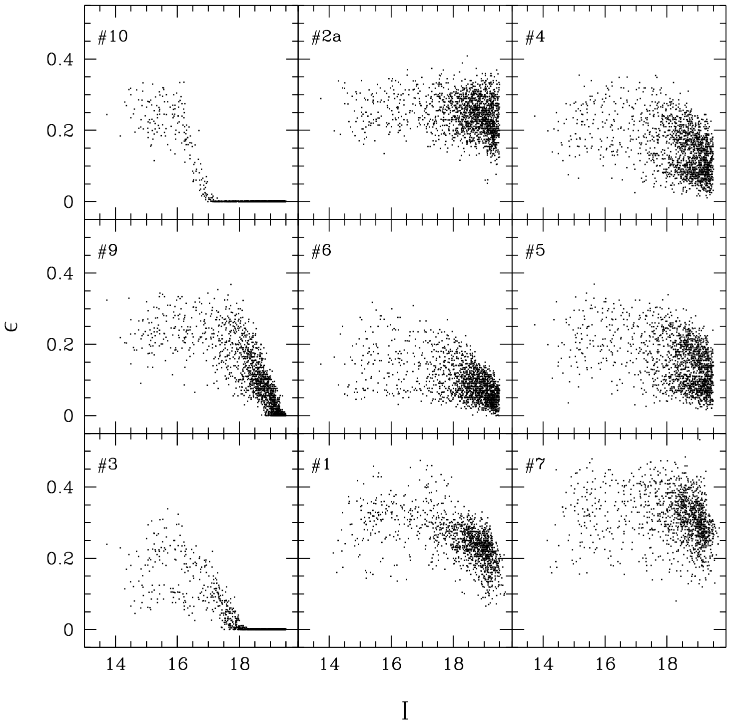

Fig. 10. The distribution of values of the efficiency parameter ϵ and the stellar I-band magnitude is shown. Notice that while I magnitude is always the same, the efficiency for a given star depends on which lens is being tested.

have good color information in our 13 fields. The final lensing candidates are shown with large circles; their distribution seems to be random and clearly belonging to the bulge population.

5.6. Color Variations

The OGLE experiment has only limited color information as most measurements were made in the I-band and only occasionally in the V-band (Udalski *et al.* 1992, 1994a). No color change was detected for any of the events, but it should be kept in mind that for many stars the colors at minimum light are uncertain, as those stars are close to the detection limit. However, the OGLE #3 event was so bright that the color was found to be constant to better than 0.02 magnitude.

6. The Optical Depth to Microlensing

Let us suppose that all microlensing events have the same time scale t_0 and that the detection efficiency is 100%. The frequency of events per year Γ is related

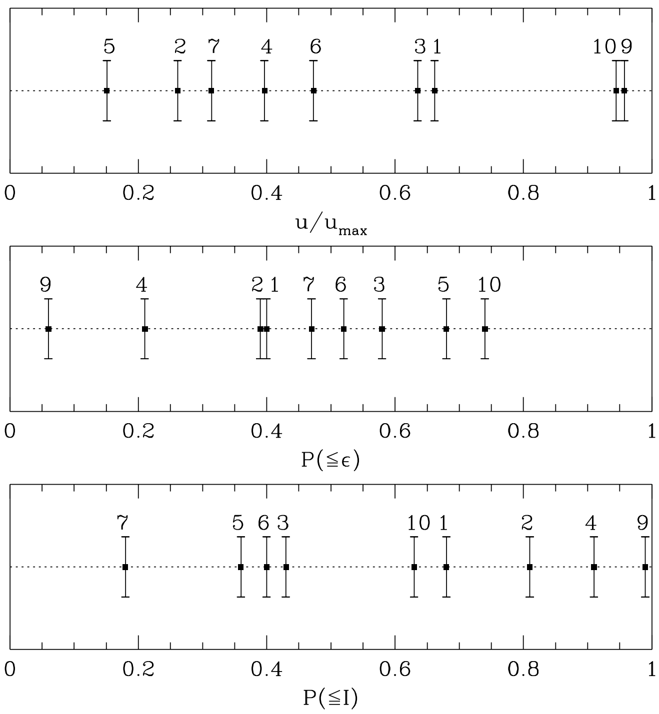

Fig. 11. The distribution of the statistical parameters for the 9 OGLE lens candidates: u/u_{max}, $P(\leq \epsilon)$, and $P(\leq I)$. The parameters are explained in Sections (5.1–5.3) and their values are listed in Table 1. The OGLE lens number is given above each bar representing the event. The events should be randomly distributed in the interval (0,1) in all three panels if the events are due to gravitational microlensing.

to the average time between the events $\langle \Delta t \rangle$ as

$$\Gamma = \frac{1 \text{ yr}}{\langle \Delta t \rangle} \tag{7}$$

and the optical depth can be calculated as (*cf* Paczyński 1986)

$$\tau = \left(\frac{\pi}{2N_m} \right) \left(\frac{t_0}{\langle \Delta t \rangle} \right), \tag{8}$$

where N_m is the number of stars that are monitored and we count only those events for which the impact parameter is smaller than the Einstein ring radius. In fact the OGLE efficiency is much less than 100% and for each event we have a different time scale t_0 and a different maximum impact parameter to which that event would be detectable. We consider the whole set of events covering the two observing seasons. Therefore, the contribution of event $\#k$ to the overall optical depth is divided by a factor of two (2 years),

$$\tau_k = \left(\frac{\pi}{2N_m} \right) \left(\frac{t_0}{\epsilon \times 2 \text{ yr}} \right) \left(\frac{1}{u_{max}} \right) \tag{9}$$

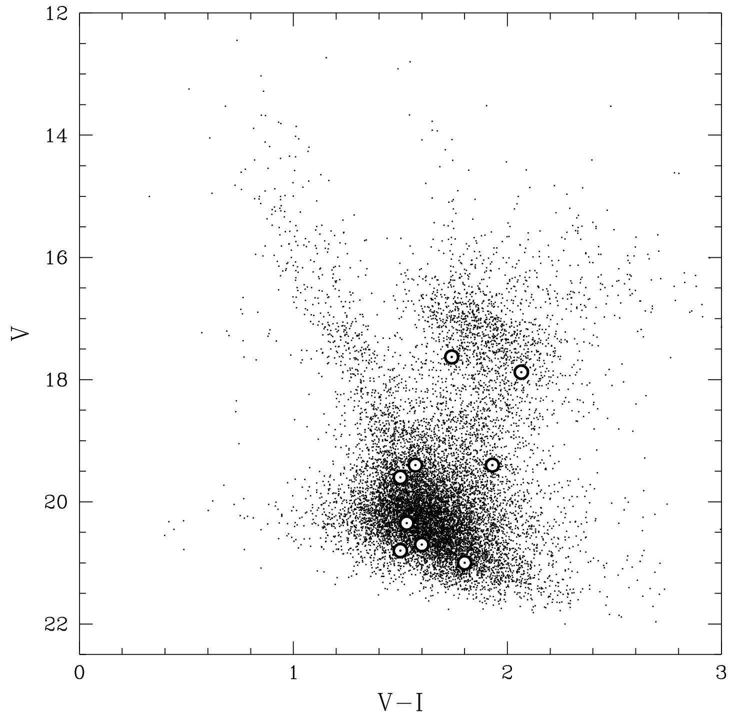

Fig. 12. The distribution of final lensing candidates (large circles) is shown in the color-magnitude diagram together with $\sim$ 12 500 stars randomly chosen from the color-magnitude diagrams of all fields. Notice the "blue main sequence" of the disk stars (*cf* Paczyński *et al.* 1994a).

where ϵ is the OGLE efficiency corresponding to the event time scale t_0, as shown in Fig. 7, N_m is the number of "constant" stars that were effectively monitored in the particular season and $u_{max} = p_{max}/R_E$.

The total number of searched for lensing constant stars with $I \leq 19.5$ was $\sim 1.4 \times 10^6$ in 1992 and $\sim 1.1 \times 10^6$ in 1993. However, these are not independent for technical reasons. First, as a consequence of PSF varying over the 2048 $\times$ 2048 CCD chip it was necessary to divide each frame into 49 sub-frames, as described by Udalski *et al.* (1992). This made some stars listed twice (sometimes more than twice) in the database and all measurements were made separately for each entry. The cross-link is available and the true number of stars has to be reduced by $\sim 12\%$ to account for the multiple listings. We have conducted the search on all listed objects and in this way the OGLE #1 has been detected twice, under two names of the same star in the same Baade's Window field BW7.

Next, there was some degree of overlap between adjacent CCD fields, as described by Udalski *et al.* (1992). This made $\sim 12\%$ of all stars measured twice as they appeared in the overlap regions. This way the OGLE #2 has been detected in Baade's Window fields BW5 and BWC (*cf* Table 1).

Finally, some stars were not in the Galactic bulge but in the Galactic disk, on average too close to be lensed. We very crudely estimate their contribution to be $\sim 5\%$, though it may be somewhat larger, as most disk stars are presumably blended with the bulge stars in the region of the color-magnitude diagram where most of all stars are located: $V \approx 20$, $V - I \approx 1.6$, as shown in Fig. 12.

All three effects combined act in the same direction: they reduce the effective number of stars searched for microlensing by a factor ~ 1.47. Therefore, the numbers to be used in evaluating the optical depth with the Eq. (9) should be $N_m \approx 0.95 \times 10^6$ in 1992 and $N_m \approx 0.75 \times 10^6$ in 1993. The contributions of the final candidate events to the optical depth (in units of 10^{-6}) are given in Table 1. The combined optical depth is $\tau \approx (3.3 \pm 1.2) \times 10^{-6}$, where the standard deviation was calculated according to the formula:

$$\sigma_\tau = \left(\sum_k (\tau_k)^2 \right)^{1/2} \tag{10}$$

Of course, this is only a random error calculated as if all events were independent. It does not allow for any systematic errors. We tried to minimize their effect but it is difficult to assess at this time how successful we were in this task.

7. Discussion

Our estimate of the optical depth to gravitational microlensing towards the Galactic bulge was made treating all 13 OGLE fields as equal. This includes 9 Baade's Window fields at $l = 1°$, $b = -4°$ and 4 Galactic Bar fields at about the same galactic latitude but at $l = \pm 5°$ (*cf* Fig. 1). If the microlensing is dominated by the Galactic bulge lenses as asserted by Kiraga and Paczyński (1994) then the expected rate should be less in Galactic Bar fields than in BW fields. Our results are consistent with this notion but they are just as consistent with the rate being the same in all fields (*cf* Table 1) as the number of events detected is small.

In order to check how our estimate of the optical depth depends on our *ad hoc* choice of the detection threshold as described in Section 2, we increased the threshold from $3\sigma_{max}$ to $8\sigma_{max}$, keeping all other rules of the algorithm the same. As expected many lenses dropped out and only 4 remained: #3, #2a, #5 and #7. The new efficiencies ϵ_k and the new values of the maximum impact parameters u_{max} were recalculated as well and the new estimate of the optical depth was obtained: $\tau = (6.8 \pm 4.4) \times 10^{-6}$. This is within one standard deviation of the estimate based on the $3\sigma_{max}$ detection threshold, indicating that the result is not sensitive to the choice of the threshold.

Our estimate of the optical depth to gravitational microlensing towards the Galactic bulge is only a lower limit. The OGLE is not sensitive to events with the time scale much less than 10 days, while in a recent theoretical model by Kiraga and Paczyński (1994) the rate of microlensing events is likely to peak at $t_0 \sim 10$ days, even if there are no brown dwarfs in the Galaxy. Also, the OGLE is not sensitive to events lasting longer than the observing seasons, with $t_0 \geq 100$ days. Such events were discriminated against with our search procedure. This would not miss many ordinary stellar mass lenses, but a significant population of dark objects with masses well above solar would be missed.

It should be pointed out that the rate of events detected by the OGLE, even though it is only a lower limit, is well in excess of any theoretical prediction todate – those were roughly in the range $0.5 \times 10^{-6} \leq \tau \leq 1.0 \times 10^{-6}$ (Paczyński 1991, Griest *et al.* 1991, Kiraga and Paczyński 1994). The discussion of the astronomical consequences of our finding will be published elsewhere (Paczyński *et al.* 1994b).

It should also be noted that many of the stars which were measured as single are in fact unresolved blends of a few stars. Notice that the seeing disk is typically $\sim 1''$, while the cross-section for gravitational microlensing is typically $\sim (0.001'')^2$. This leaves plenty of room for unresolved blends of which only one is to be lensed. If that happens the amplitude as measured is reduced and the impact parameter for the lensing is overestimated. In addition, our experience with improved photometry (Udalski *et al.* 1994a) indicates that with the corrected stellar position the amplitudes turns out to be larger, *i.e.* in the original database photometry the amplitudes are underestimated and the impact parameters are overestimated. Both effects act in the same direction and lead to underestimate of the actual number of lensing events and to underestimate of the optical depth to microlensing. We have made no quantitative assessment of this effect, but it can only increase even more the apparent discrepancy between the observation and currently available models.

Photometry of the OGLE microlensing events, as well as a regularly updated OGLE status report can be found over the Internet from sirius.astrouw.edu.pl host (148.81.8.1), using the anonymous ftp service (directory "/ogle", files "README", "ogle.status"). The report contains the latest news and references to all OGLE related papers and the PostScript files of some publications, including this one. Information on the recent OGLE status is also available via "World Wide Web" WWW: "http://www.astrouw.edu.pl/".

Acknowledgements. This project was supported with the NSF grants AST 9216494 and AST 9216830 to B. Paczyński and Polish KBN grants No 2-1173-9101 and BST475/A/94 to M. Kubiak.

REFERENCES

Griest, K., *et al.* 1991, *Astrophys. J. Letters*, **372**, L79.
Kiraga, M., and Paczyński, B. 1994, *Astrophys. J. Letters*, in press.
Lupton, R.H., Fall, S.M., Freeman, K.C., and Elson, R.A.W. 1989, *Astrophys. J.*, **370**, 201.
Mao, S., and DiStefano, R. 1994, *ApJ*, submitted.
Paczyński, B. 1986, *Astrophys. J.*, **304**, 1.
Paczyński, B. 1991, *Astrophys. J. Letters*, **371**, L63.

Paczyński, B., Stanek, K.Z., Udalski, A., Szymański, M., Kałużny, J., Kubiak, M., and Mateo, M. 1994a, *Astron. J.*, **107**, 2060.

Paczyński, B., Stanek, K.Z., Udalski, A., Szymański, M., Kałużny, J., Kubiak, M., Mateo, M., and Krzemiński, W. 1994b, *Astrophys. J. Letters*, submitted.

Schechter, P.L., Mateo, M., and Saha, A. 1993, *P.A.S.P.*, **105**, 1342.

Schmidt, M. 1968, *Astrophys. J.*, **151**, 393.

Szymański, M., and Udalski, A. 1993, *Acta Astr.*, **43**, 91.

Udalski, A., Szymański, M., Kałużny, J., Kubiak, M., and Mateo, M. 1992, *Acta Astr.*, **42**, 253.

Udalski, A., Szymański, M., Kałużny, J., Kubiak, M., and Mateo, M. 1993a, *Acta Astr.*, **43**, 69.

Udalski, A., Szymański, M., Kałużny, J., Kubiak, M., Krzemiński, W., Mateo, M., Preston, G.W., and Paczyński, B. 1993b, *Acta Astr.*, **43**, 289.

Udalski, A., Szymański, M., Kałużny, J., Kubiak, M., Mateo, M., and Krzemiński, W. 1994a, *Astrophys. J. Letters*, **426**, L69.

Udalski, A., Szymański, M., Mao, S., Kałużny, J., Kubiak, M., Mateo, M., and Krzemiński, W. 1994b, in preparation.